29th EPS Conference on Plasma Phys. and Contr. Fusion Montreux, 17-21 June 2002 ECA Vol. **26B**, P-1.044 (2002)

Advanced high field side pellet refuelling and mitigation of ELM effects in ASDEX Upgrade

P.T. Lang*, M. Reich, R. Dux, T. Eich, L. Fattorini[1], J.C. Fuchs, O. Gehre, J. Gafert, A. Herrmann, M. Jacobi, M. Kaufmann, S. Kálvin[2], G. Kocsis[2], B. Kurzan, M.E. Manso[1], V. Mertens, H.W. Müller, H.D. Murmann, J. Neuhauser, I. Nunes[1], D. Reich[3], K.F. Renk[4], W. Sandmann, J. Stober, U. Vogl[3], ASDEX Upgrade Team

Max-Planck-Institut für Plasmaphysik, EURATOM Association, Boltzmannstr. 2, 85748 Garching, Germany
[1] *Centro de Fusão Nuclear, Associacão EURATOM/IST, Instituto Superior Técnico, 1046-001 Lisboa, Portugal*
[2] *KFKI Research Institute, P.O. Box 49, 1525 Budapest, Hungary*
[3] *Fachhochschule Amberg-Weiden, Kaiser-Wilhelm-Ring 23, 92224 Amberg, Germany*
[4] *Institut für Experimentelle und Angewandte Physik, NWF II, Universität, 93040 Regensburg, Germany*
* *Corresponding author; e-mail: ptl@ipp.mpg.de*

1. Introduction

For the ITER-FEAT project the reference scenario to achieve extended fusion power is still inductive operation in the type-I ELMy mode. To achieve extended experimental headroom, high density operation seems to be desirable [1]. Thus, the pellet injection tool launching small mm to cm sized bodies composed of frozen fuel into the plasma might offer solutions for two major concerns of ITER-FEAT: (i) efficient plasma particle fuelling to achieve high density, and (ii) ELM controlling and mitigation. Advanced pellet refuelling requires high efficiency while maintaining good plasma confinement, achieved only with sufficiently deep pellet penetration which minimises edge losses. As demonstrated in many tokamaks, pellet launch from the magnetic high field side (HFS) shows the best performance regarding this criterion. Consequently, a HFS pellet injection system is considered for ITER-FEAT. For the proper layout of such a system sufficiently accurate prediction of pellet penetration is essential. Since a modelling tool serving for this task is not yet available, an empirical penetration scaling for HFS pellet injection is helpful. Collecting data from ASDEX Upgrade experiments spanning a parameter range as wide as available, we derived a first approach for such an empirical regression approach. Also, a framing camera system yielding high temporal and spatial resolution was set into operation. Dedicated for a detailed study of the ablation process, the system already started to deliver first data. A first experimental approach for controlled triggering of ELM events was undertaken at ASDEX Upgrade. To test the possibility of releasing ELMs at a rate higher than the natural rate, long sequences of pellets were launched. Since our system is currently optimised for refuelling experiments, restrictions on the pellet rate were necessary in order to avoid strong density increase. Despite this fact very encouraging results were obtained.

2. Experimental setup

The final set up of the looping pellet injection system for high field side launch is now in operation at ASDEX Upgrade. The system allows pellet injection at rates up to 75 Hz and velocities ranging from 240 m/s to about 900 m/s. Launched from the inner side of the torus, the pellets' designated injection path aims towards the plasma centre tilted at a poloidal angle of 72° with respect to the horizontal midplane. Doping the pellets with small amounts of Nitrogen was used to restrict pellet mass losses which are caused by the transfer in the guiding tube and increased with velocity.

A fast camera system was installed for pellet observation from the top, allowing for high spatial ($\simeq mm$) and temporal ($\simeq \mu s$) resolution. The pellet injection setup as well as the framing camera observation geometry are displayed in fig. 1. Several conventional video camera systems yielding frames integrating over the full duration of a single pellet's ablation as well as several diodes recording time resolved signals of the ablation emission were employed to determine the absolute pellet penetration depths δ. Furthermore, a full set of diagnostics was in operation, some run in an adapted setting to record density and temperature profiles at high temporal resolution. This way, density and temperature profile evolution during and after pellet injection could be visualised.
In the experiments target plasmas were run in the lower single null divertor configuration with elongation of typically $\kappa = 1.6$ but with a large variety in plasma current, toroidal field and applied heating power. For auxiliary heating, D_0 NB injection and ICRH was employed.

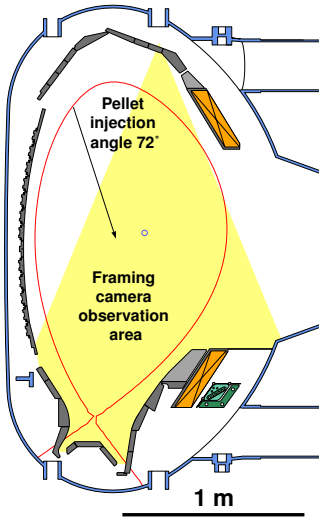

Figure 1: *Poloidal cross section of ASDEX Upgrade with pellet injection and framing camera observation geometry. Separatrix of a typical plasma configuration shown as well.*

3. Results

3.1. HFS pellet penetration scaling using ASDEX Upgrade data

For reliable application of the pellet tool, precise prediction of several aspects of pellet injection is necessary. At present, a fully compatible theory for determining penetration depth and possibly also mass deposition from pellet injection has not yet been established. The IPADBASE[2] approach has shown that for low field side pellets an empirical scaling law is suitable for estimating pellet penetration depths in different machines. It has been used as a guideline to study the penetration depth of ASDEX Upgrade HFS pellets. Since pellets rarely penetrate to the centre, and edge effects are relevant for pellet penetration, the temperature variable was - in contrast to the IPAD approach - not taken from central temperature, but $W_{mhd} = nkT$ was used as a measure for the plasma temperature.

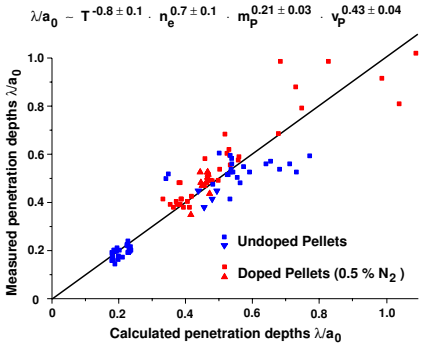

Figure 2: *Regression analysis for HFS pellet penetration.*

A wide range of plasma and pellet parameters was explored while restricting the regression analysis to the most important factors. It was assumed that plasma current, temperature and density as well as the applied magnetic field are the dominant influencing factors. No attention was payed to q-profile, elongation and triangularity at this stage. While temperature and density varied strongly over the dataset, B_t and I_p did not scatter enough to justify a more complicated model. Pellet parameters that presumably influence the penetration depth are mass, velocity and doping. The latter was only evaluated after the

regression and not used as a free variable. The penetration depth was measured using video, where the full ablation trace is recorded into one frame as well as by velocity based analysis of the ablation light time trace.
Using the full set of pellets (including doped ones) a standard regression analysis was performed to get exponents of the empirical formula $\lambda/a_0 = C \cdot T^a \cdot n_e^b \cdot m_P^c \cdot v_P^d$. Results are shown in fig. 2, where the measured penetration depth in normalised units (λ/a_0) is plotted over the penetration depth calculated with the empirical formula using the parameters derived in the regression. While n_e and T can not be regarded absolutely independent of each other, most likely the ($n_e \cdot T$) exponent would be correct, for a better comparability with the IPAD approach, the distinction was used. Looking at the numbers, one can see a similar scaling law for HFS as for LFS, but the absolute numbers are enhanced by a factor of 2-3 on the HFS. Doped pellets show a small but significantly deeper penetration for same scaling values than their undoped counterparts. The hardening effect by Nitrogen doping also has a very positive effect on attainable velocities and therefore increases potential penetration by an even higher amount.

3.2. First observations with the fast framing camera

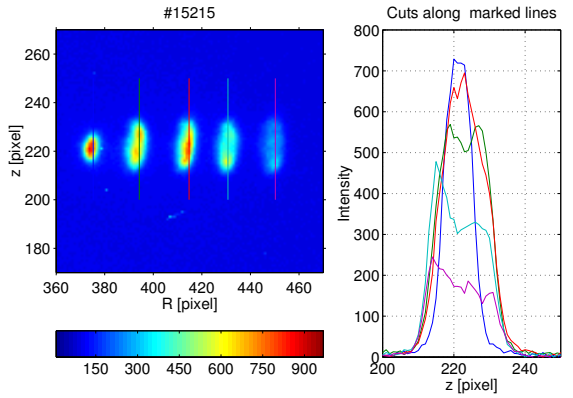

Figure 3: *Framing camera image made in multiple exposure (5 μs exposures with 62.5 μs separation) mode about D pellet (≃ 7.2mm³) with 600 m/s velocity. The individual cigar shaped patches represent images of the pellet cloud radiation at different times.*

In order to get deeper insight into physics of pellet ablation and interplay between plasmoid drift and penetration, detailed modelling is required. For testing of theoretical models observation of the ablation cloud with high spatio-temporal resolution is needed to follow the evolution of the pellet cloud. For this purpose we developed an observation system based on a fast framing camera. As a first result a multiple exposure image is presented in fig. 3. From this type of images one can conclude that (i) the size of the pellet cloud perpendicular to the magnetic field lines is in the order of cm, (ii) the cloud distribution along the field lines can be peaked and hollow as well. In future, detailed investigations for variations in all important pellet and plasma parameters are foreseen.

3.3. Active ELM controlling aiming at mitigation of ELM effects

During previous experiments with pellets applied for particle refuelling it turned out that injection during ELMy H-mode phases resulted in the almost immediate trigger of an ELM event by the pellet. However, refuelling pellets yielding significant increase of the initial plasma density often cause a burst of ELMs stronger and longer than natural background ELMs during the post-pellet phase. Reduction of pellet sizes performed for this experimental investigation showed that the instant ELM remains but the following ELM burst attenuates with the pellet mass reduction. When pellet sizes sufficiently small are used a pellet essentially results in the instant release of only one additional ELM event causing particle and energy loss comparable to typical type-I background ELMs. Unfortunately our injection system built for refuelling purposes can only sporadically deliver pellets of such small sizes. Long lasting pellet trains with high delivery reliability for every single pellet as required for a suitable persistent ELM control approach had

to be composed of pellets clearly oversized for the intended task. While pellet induced ELM losses still were dominated by the instant ELM for these injector settings, notable density enhancement was faced. Restricting pellet induced density increase to 10% the initial value limited the pellet rate to 20 Hz. Suitable target discharges required for a demonstration of successful ELM control by pellets therefore must provide a significantly lower natural ELM frequency. Therefore we chose a plasma configuration with $I_P = 1MA$, $B_t = 2T$, $q_{95} = 3.8$ and a medium triangularity and applied auxiliary heating of 1.5 MW NI and 2.3 MW central ICRH.
The selected heating power was just sufficient to enter the type-I ELM regime with the central power deposition by the ICRH preventing peaking of the density profile and hence occurrence of neoclassical tearing modes [3]. Reference discharges of this type evolved into a steady phase with strong ELM events occurring regularly at about 3 Hz lasting for about 4.8 s until the end of the heating phase. Yielding already a suitable target for the control approach, the final reference discharge got an additional mild gas puff driving up the density to the same level as the pellet controlled discharge. The impact of pellet controlling (15520, red) with respect to this most similar reference shot (15420, blue) is visualised in fig. 4. Clearly, the ELM frequency now equals the pellet rate as every pellet triggers an ELM and every ELM during the pellet sequence is triggered by a pellet. Thus, pellet controlling indeed increases the ELM frequency from 3 to 18.8 Hz.

Pellet induced ELMs show a signature with respect to particle and energy losses as well as duration and power load to the divertor plates like those found for natural ELMs of same frequency ($\simeq$ 20 Hz) in comparable discharges. Furthermore, the ratio $\frac{\Delta W_{ELM}}{W_{mhd} \times f_{ELM}}$ (ΔW_{ELM} energy loss per ELM, f_{ELM} ELM frequency) remains constant and relative ELM energy losses with respect to the normalised ELM frequency fit well to the scaling found in JET and ASDEX Upgrade [4]. Of course this experimental approach requires an extention towards even higher ELM frequencies since background ELM frequencies have been peculiarly low in these experiments. Such an extention however needs an injection system better adapted to the specific needs for ELM control with minimal side effects. Nevertheless the presented first test already shows that pellet injection seems to be a feasible option for ELM control and, if near total control can be achieved, also the much desired mitigation of ELM effects might succeed.

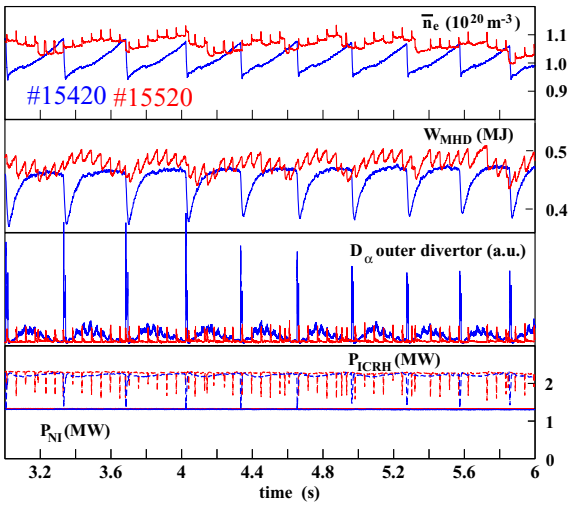

Figure 4: *Demonstration of controlled ELM triggering by pellet injection. Persisting injection of a continuous pellet train increases the ELM frequency from 3 Hz observed in a reference discharge (15420, blue) to the pellet rate (18.8 Hz in 15520, red). With pellet initiated ELM controlling, density and energy evolution becomes clearly smoothened by mitigating particle and energy losses per ELM*

References

[1] Y. Shimomura et al., Nucl. Fusion, **41** 309 (2001).
[2] L. Baylor et al., Nuclear Fusion **37** 1133 (1997).
[3] J. Stober et al., Nuclear Fusion **41** 1535 (2001).
[4] A. Herrmann, Plasma Phys. Control. Fusion **44** 1 (2002).